Enhanced Performance of Organic Light Emitting Device by Dual Doping of LiF in ETL and HTL

Yaqin Liao and Xingyuan Liu

J. Electrochem. Soc. 2010, Volume 157, Issue 7, Pages H759-H762.
doi: 10.1149/1.3428372

Journal of The Electrochemical Society, **157** (7) H759-H762 (2010)
0013-4651/2010/157(7)/H759/4/$28.00 © The Electrochemical Society

Enhanced Performance of Organic Light Emitting Device by Dual Doping of LiF in ETL and HTL

Yaqin Liao[a,b] **and Xingyuan Liu**[a,z]

[a]*Key Laboratory of Excited State Processes, Changchun Institute of Optics, Fine Mechanics and Physics, Chinese Academy of Sciences, Changchun 130033, People's Republic of China*
[b]*Graduate School of Chinese Academy of Sciences, Beijing 100080, People's Republic of China*

In this paper, we demonstrated an organic light emitting device based on both lithium fluoride (LiF)-doped hole transporting layer (HTL) and electron transporting layer (ETL). The optimization LiF dual doping device shows dramatic improved luminance and current efficiency. The maximum luminance and current efficiency are 28,180 cd/m^2 and 4.7 cd/A, respectively, for the dual doping device and 12,320 cd/m^2 and 3.7 cd/A, respectively, for the traditional LiF/Al cathode device. Furthermore, the maximum current efficiency shows a decline proportion of 25% for the LiF dual doping device and 46% for the traditional LiF/Al cathode device. Such improved properties are attributed to the enhanced carrier transporting and balanced numbers of holes and electrons injected into the emitter layer by LiF dual-doped HTL and ETL.
 [DOI: 10.1149/1.3428372]

Manuscript submitted November 3, 2009; revised manuscript received March 25, 2010. Published May 21, 2010.

The low operating voltage and high efficiency not only promote the commercialization of organic light emitting devices (OLEDs) but also favor to improve the performance of electrically pumped organic lasers (OLDs)[1,2] (because the stable high device efficiency and the low operating voltage are the key factors to achieve gain and lasing for OLDs). However, for the few intrinsic carrier concentrations,[3] low mobility of organic semiconductors, and the unmatched energy level of the electrode interface,[4] the operating voltages of OLEDs are still much higher than those of their inorganic competitors. To lower the driving voltage and improve the current efficiency (CE) of OLEDs, it is necessary to enhance the carrier injection and transporting and balance the numbers of holes and electrons injected into the light emitting layer (EML). The current density is mainly determined by the carrier mobility and the ability of the carrier injection from the electrode to the organic layer,[5] and the luminance is greatly dependent on the recombination efficiency of holes and electrons.

Doping with strong electron acceptor materials such as tetrafluorotetracyanoquinodimethane[6] in a hole transporting layer (HTL) and donor materials such as alkaline metal[5,7,8] in an electron transporting layer (ETL) have proved to be the most effective way to strengthen the carrier injection and transporting. However, the alkaline metals are well known to have negative influence on device stability and that they are easier to diffuse into ETL, resulting in the quenching of excitons in the organic EML. To solve these problems, recently, metal oxides such as MoO_3,[9] MoO_2,[10] WO_3,[11] ReO_2,[12] and MnO [13] have been reported to act as dopants for HTL or injection layer. The alkali metallic fluorides (e.g., LiF,[14] NaCl,[15] CsF,[16] and NaF [17]) are also used as the dopants for ETL or injection layer. Especially, LiF has effectively improved the device performance by doping in ETL.[18,19] Nevertheless, there are still some problems. Although the doping of LiF could greatly improve the device performances by changing the doping ratio, the highest CE, which descended rapidly, was still achieved at a very low current density (only several tens of mA/cm^2).[18] This indicates that the concentrations of holes and electrons are unbalanced at a high current density in these devices, which is extremely unbeneficial to achieve gain in OLDs and helpless for commercial applications.

In this paper, LiF was introduced as both the ETL and HTL dopants. The electron transporting ability of ETL could be dramatically enhanced by LiF-doped ETL, and the balance of holes and electrons injected into the EML could be greatly improved by LiF-doped HTL. Consequently, a low driving voltage and high luminance OLED with an improved stability in CE was achieved by optimized LiF doping ratios in ETL and HTL. The optimization dual LiF doping device shows a doubled brightness and the balanced CE at a large current density range, compared with those of traditional Al/LiF cathode devices.

[z] E-mail: xingyuanliu@hotmail.com

Experimental

All device configurations are detailed in Fig. 1. In this study, the doping ratio was the volume ratio. The device shown in Fig. 1a was named as the LiF/Al cathode device (device A). The devices shown in Fig. 1b were named as LiF-ETL doping devices; the doping ratios were 3% (device B), 4.5% (device C), and 6.5% (device D). The devices shown in Fig. 1c were named as dual doping devices; the doping ratios of LiF in ETL were all 4.5%, and the doping ratios of LiF in HTL were 4.5% (device E), 8% (device F), and 15% (device G). A glass substrate coated with 110 nm thick indium tin oxide (ITO) with a sheet resistance of 100 Ω/□ was used as an anode. The cleaned ITO substrates were set in the vacuum chamber and treated with O_2 plasma 3 min at a power of 50 W. All organic materials were obtained commercially and deposited by vapor deposition under 5.0×10^{-4} Pa according to the sequence described in Fig. 1. The evaporation rates of LiF, Alq, and *N*,*N*′-diphenyl-*N*,*N*′-bis(1-naphthyl-(1,1′-biphenyl)-4,4′-diamine (NPB) were strictly controlled using three oscillating quartz thickness monitors. LiF-doped organic layers were formed by coevaporation of LiF and organic materials from separate sources. Every source has a separateness probe to detect the evaporation rates of materials. The doping uniformity of the LiF-doped organic layers should be promised by the accurate evaporation rates of every material in macroscopic. The typical rate of the deposition of NPB and Alq was 2 Å/s. The depositing rate of LiF in the LiF/Al cathode device was 0.5 Å/s. The Al cathode was deposited under 4.0×10^{-4}–1.0×10^{-4} Pa with an evaporation rate of 10 Å/s. All devices had the same active area of 4 mm^2. The film thickness was measured with an Ambios XP-1 surface profiler. The current–voltage characteristics were measured with a Keithley 2400 source meter. The electroluminescence (EL) spectra and luminance were recorded with a PR705 Photo Research spectrophotometer. All the tests were carried out in air at room temperature.

Results and Discussion

To investigate the influences of LiF on carrier injection and transporting, the OLEDs based on LiF-doped ETL with various doping concentrations had been fabricated. Figure 2a shows the current density–voltage (*J*-*V*) characteristics of the LiF-ETL doping devices. An obvious reduction in driving voltage at the same current density in the LiF-ETL doping device with higher doping concentrations (devices C and D) could be observed, compared with that of device A. Furthermore, devices C and D show the maximum current densities as high as 1050 and 1000 mA/cm^2, respectively. Com-

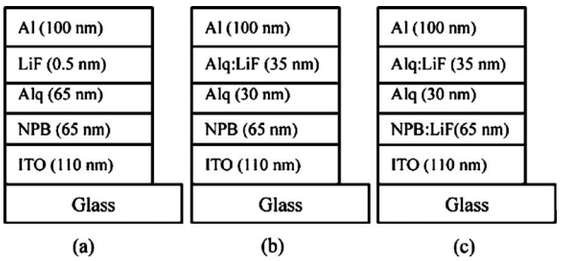

Figure 1. Configurations of multilayer OLEDs: (a) LiF/Al cathode device (device A); (b) LiF-ETL doping device devices [doping ratio: 3% (device B), 4.5% (device C), and 6.5% (device D)]; and (c) dual doping devices [doping ratio in ETL is 4.5% and doping ratios in HTL: 4.5% (device E), 8%(device F), and 12% (device G)].

pared with those of devices A and B (600 mA/cm^2), the maximum current density is improved nearly 70%. This indicates that the electron transport ability of the Alq layer is greatly enhanced by LiF doping when the doping ratios are higher than 4.0%. Nevertheless, the LiF-ETL doping devices show little evident enhancement in carrier injection abilities (for the turn-on voltage is proportional with the carrier injection ability), compared with the LiF/Al cathode device (device A) (Table I). Without the LiF buffer layer, the Alq/Al device normally has a turn-on voltage of ~7 V.[13] The insertion of a LiF thin layer (0.5–1.0 nm) between Alq/Al dramatically improves the electron injection ability from the cathode Al to the Alq layer (ETL). Although the effect is not obvious in LiF-ETL doping devices, the changing trend of turn-on voltage in devices B, C, and D suggests that higher LiF doping ratios are in favor of decreasing the barrier height between the cathode and the ETL, resulting in better electron injection than the LiF/Al cathode device. The lower doping ratio device (device B) shows the poorest *J-V* characteristic and the highest turn-on voltage, which indicates that a lower LiF doping ratio could not efficiently improve the electron injection and possibly would decrease the mobility of electrons in ETL due to the trap effect.

Figure 2b and c shows the current efficiency–current density (CE-*J*) and the luminance–current density (*L-J*) characteristics of the LiF-ETL devices. Device B has the maximal CE of 4.6 cd/A at only 30 mA/cm^2. However, the rapidly declining CE with current density results in an inferior brightness (14,410 cd/m^2) compared with those of devices C and D. Despite the nonideal CEs, the heavier doping LiF-ETL devices exhibit outstanding performance on luminance, which is 27,490 cd/m^2 for device C and 21,930 cd/m^2 for device D. It could be attributed to the stability of the CE in devices C and D, as shown in Fig. 2b. Although some of the maximal CEs of devices C and D were lower than those of devices A and B, the CEs in devices C and D were almost holding constant at the whole current density range. This character promised good performance of devices C and D on luminance at the high current density.

Extremely high current density and low CE in devices C and D reveal that the balance of the numbers of holes and electrons injected into the Alq layer should be further improved. Figure 2 shows that the 4.5% LiF-ETL doping device (device C) represents superior *J-V*, *L-J*, and CE-*J* properties. Since then, 4.5% is regarded as an optimization ETL doping ratio in this study, which is immovable in all dual doping devices. The balance of holes and electrons has been investigated by varying the doping ratios of LiF in NPB (HTL). Figure 3 shows the *J-V*, CE-*J*, and *L-J* characteristics of dual doping devices E, F, and G. It was found in Fig. 3a that with the rising of the LiF-HTL doping ratios, the carrier density under the same voltage is dropped and the turn-on voltage (Table I) is increased. This can be attributed to the fact that the hole numbers injected from ITO to NPB is reduced for the heightened barrier height between the anode and HTL interface. We conducted an indirect experiment to validate it. The work functions of ITO and ITO/LiF (0.5 nm) were

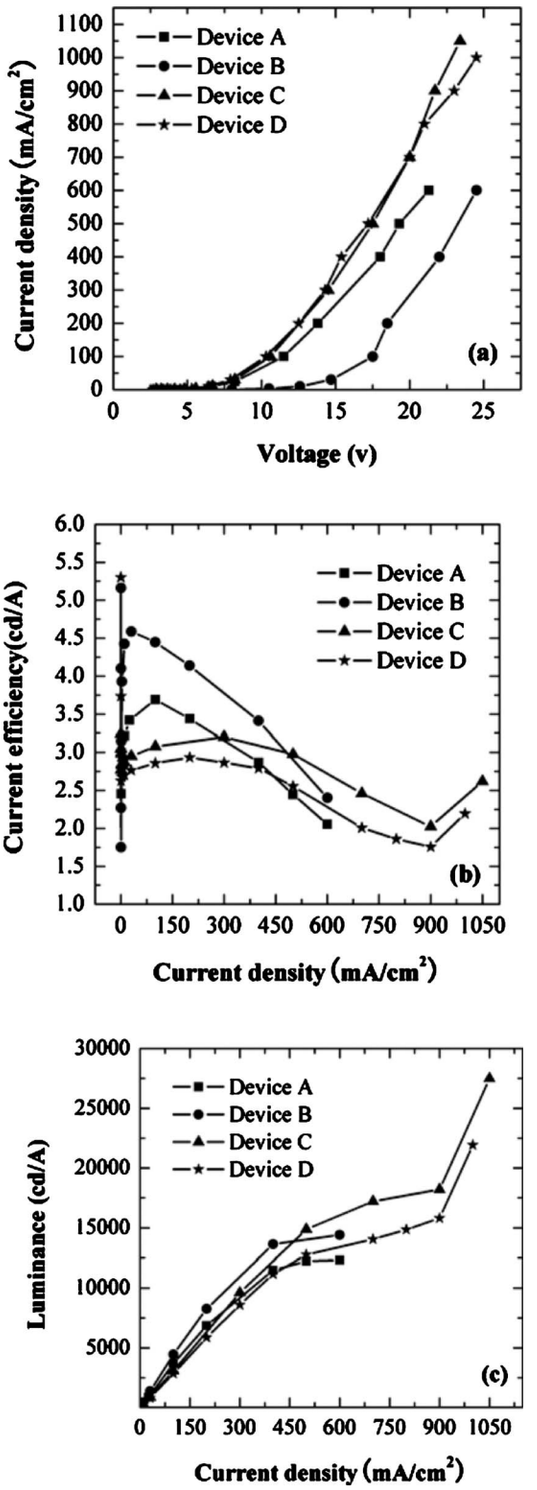

Figure 2. (a) *J-V*, (b) CE-*J*, and (c) *L-J* characteristics of devices A, B, C, and D.

measured by an ambient Kelvin probe. The results show that the ITO work function falls from −4.8 to −4.6 eV by covering with a 0.5 nm thick LiF ultrathin film.

Figure 3b shows that the stability of CE is not influenced by the LiF-HTL doping, and all the dual doping devices represent a higher CE than that of device C. It indicated that LiF doped in HTL could

Table I. EL properties of devices.

Device	Turn on voltage at 1 cd/m^2 (V)	Maximum current density (mA/cm^2)	Maximum luminance (cd/m^2)	Maximum CE (cd/A)	Decline proportion of maximum CE (%)
A	3.0	600	12,320	3.7 cd/A at 100 mA/cm^2	46
B	3.4	600	14,410	4.6 cd/A at 30 mA/cm^2	48
C	3.1	1050	27,490	3.2 cd/A at 300 mA/cm^2	19
D	2.9	1000	21,930	2.9 cd/A at 200 mA/cm^2	25
E	3.0	800	28,180	4.7 cd/A at 200 mA/cm^2	24
F	4.4	800	22,110	3.7 cd/A at 200 mA/cm^2	24
G	8.2	700	18,970	3.7 cd/A at 100 mA/cm^2	27

improve the number balance of holes and electrons injected into the EML. Compared with that of device C, the maximum luminance of devices F and G is still inferior, which can be induced by the relatively low current densities of devices F and G under higher voltage. Device E shows a maximum CE of 4.7 cd/A and a maximum luminance of 28,180 cd/m^2 for the significantly improved carrier balance compensated to the loss induced by the lower current density and hole injection.

From Fig. 2 and 3 and Table I, it can be deduced that, first, LiF-ETL doping devices have no obvious improvement on turn-on voltage compared with the LiF/Al cathode device, but the electron mobility in Alq can be significant increased by raising the LiF doping ratios. Second, the hole injection ability is in inverse proportion to the ratios of LiF-HTL, but the hole mobility of heavier ratio LiF-HTL-doped devices can be enhanced at the high electrical field, for the suddenly ascending curve slopes of devices F and G at the high electrical field could be observed in Fig. 3a. Finally, it indicates that the number balance of holes and electrons injected into the light EML can be dramatically improved by optimizing the LiF doping ratios in ETL and HTL. For example, the 4.5% LiF-HTL doping ratio has little influence on the turn-on voltage compared with the LiF/Al cathode device, but it balanced the carrier concentrations effectively. Therefore, device E shows the best CE-*J* and *L*-*J* properties and the stable CE.

Photoelectron emission measurements have shown that LiF can lower the energy levels of Alq [14] and the LiF-doped Alq film shows a weak n-doping effect.[20] The influence of LiF doping has been attributed to the high dielectric constant of LiF (9.036).[21] According to Maxwell's equations, the high dielectric of LiF would lead to great polarizability. When the LiF dipoles are uniformly doped in organic materials, they probably have a distribution of alignments, as illustrated in Fig. 4. With the alignments of LiF dipoles, the dielectric of organic materials increases.[22] Assuming that the dipole moments are in the same magnitude as p, the dipole alignments give an additional polarizability to organic materials from the Langevin theory

$$\chi_L = \frac{P^2}{3\kappa_B T} \quad [1]$$

$$\varepsilon = \frac{3 + 2\alpha\chi_L}{3 - \alpha\chi_L} \quad [2]$$

This additional polarizability increases the dielectric constant of the organic materials. The maximum current density that a depleted, trap-free semiconductor with thickness L can carry as space-charge limited (SCL) and given by the Mott–Gurney law is[23]

$$J_{SCL} = \left(\frac{9}{8}\right)\varepsilon\varepsilon_0\mu V^2/L^3 \quad [3]$$

where ε is the dielectric constant, μ is the charge carrier mobility, and V is the applied voltage. By definition, an ohmic contact poses no limitation to the current flow and therefore supplies the semiconductor with SCL current. Otherwise, if the supply from the contact is not adequate to satisfy the demand of the bulk, the contact is injection-limited and the current is lower than J_{SCL}. Although there is no ideal ohmic contact and trap-free device, the law is still helpful to analyze the characteristics of current density, carrier injection, and transporting. Clearly, J_{SCL} is proportional to dielectric constant. Upon that, the electron and hole transport properties of organic materials can be improved by LiF doping.

The carrier injection is limited by an interfacial energy barrier (Φ_b). Because of the image force, Φ_b depends on the electric field at the interface

$$\Phi_b = \Phi - e\sqrt{\frac{e|E_{L,R}|}{\varepsilon}} \quad [4]$$

where Φ is the Schottky energy barrier at zero field, $E_{L,R}$ is the electric field at the left (or right) contact, and ε is the dielectric constant. The cathode barrier height decreases and the anode barrier height increases with the increase in the dielectric constant. The lowest unoccupied molecular orbital energy level of Alq is −3.3 eV. The work function of Al is −4.3 eV. The highest occupied molecular orbital energy level of NPB is −5.4 eV, and the work function of ITO is −4.8 eV. The decreased barrier height is helpful for electron injection, but the hole injection is impeditive by the increased barrier height. Therefore, the turn-on voltage is proportional to the LiF-ETL doping ratios and inverse proportional to the LiF-HTL doping ratios. For the similar reason, the lower hole injection ability of devices F and G leads to the descending of current density and luminance in comparison with device C. The theoretical analysis is greatly consistent with the experiment analysis in other papers.[5,20]

The stable high CE of the dual LiF doping device and the slightly changed CE of the 4.5 and 6.5% LiF-ETL doping devices could also be explained by the contribution of the high dielectric constant of LiF.[24] According to Ohm's law, the high dielectric constant of LiF facilitates a rising in resistance, which induced an increase in the electric field of organic transporting films. The field dependence carrier mobility of amorphous organic films is often adopted in the following form

$$\mu = \mu_0 \exp\left(\sqrt{\frac{E}{E_0}}\right) \quad [5]$$

where μ_0 is the zero-field mobility and E_0 is a characteristic parameter to be determined experimentally. Clearly, the carrier mobility is proportional to the electric field. The enhanced carrier mobility at the higher voltage could promote a growth in recombination, which improves the luminance of devices and keeps the CE at a large range of current density. If the device could balance the hole and electron, it performs excellently both in CE and luminance characteristics as device E has done. The mediocre performances in the CE of the 4.5 and 6.5% ETL doping devices at a lower voltage are possibly due to the unbalance of holes and electrons and the effect of traps for the higher concentration of LiF. The balance of holes and electrons is enhanced by the increase in electric field as discussed above. Furthermore, the increase in carrier mobility as Eq. 5 described offsets the negative influence of traps, which results in the good performance in the stability of CE and the luminance of the higher doping

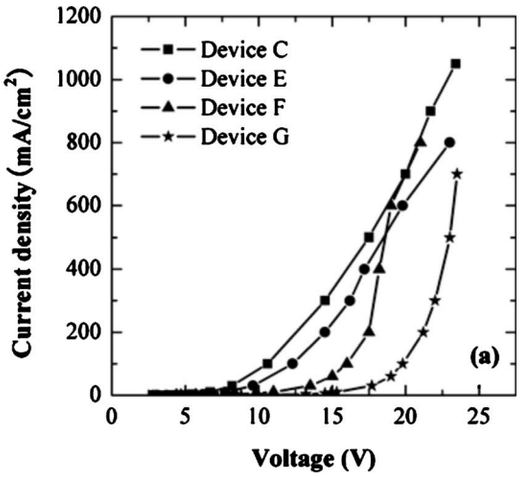

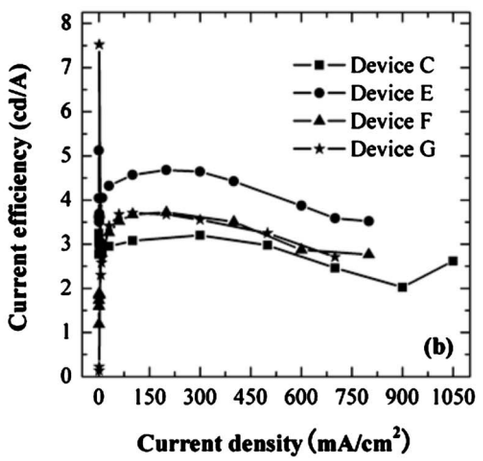

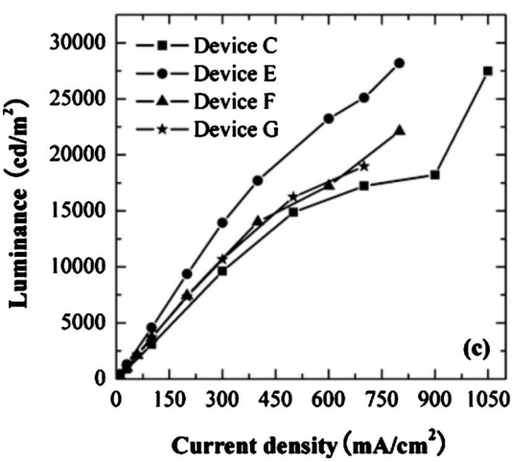

Figure 3. (a) *J-V*, (b) CE-*J*, and (c) *L-J* characteristics of devices C, E, F, and G.

ratio devices. Devices F and G exhibit bad *J-V* properties at a lower electric field, resulting from the poor hole injection induced by the higher LiF-HTL doping ratios. The steep *J-V* curve slopes, shown in Fig. 3a, suggest that the hole mobility is enhanced with the increase in the electric field. Consequently, the carrier balance of devices F and G is improved by the enhanced hole mobility, and the stability of CE could be promised.

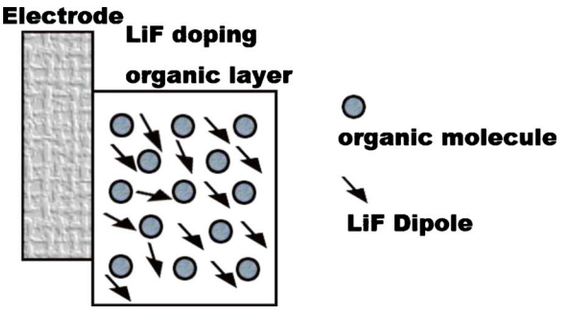

Figure 4. (Color online) The model of LiF dipole alignments.

Conclusions

In the present study, a facile nonalkaline dual LiF doping device, both doped in ETL and HTL, has been demonstrated. The optimized dual doping device leads to a great enhancement in carrier balance, carrier transporting, CE, and its stability with current density. This is quite useful for the development of organic electrical pumping laser. The stable insulator LiF as a doping material could eliminate the problem of the oxidation of reactive alkali metal dopants. The simple device structures are in favor of the improvement of EL properties of OLEDs.

Acknowledgments

This work was supported by the CAS Innovation Program and Jilin province Science and Technology Research project no. 20090346.

Chinese Academy of Sciences assisted in meeting the publication costs of this article.

References

1. M. A. Baldo, R. J. Holmes, and S. R. Forrest, *Phys. Rev. B*, **66**, 035321 (2002).
2. X. Y. Liu, H. B. Li, C. Y. Song, Y. Q. Liao, and M. M. Tian, *Opt. Lett.*, **34**, 503 (2009).
3. P. E. Burrows, Z. Shen, V. Bulovic, D. M. McCarty, S. R. Forrest, J. A. Cronin, and M. E. Thompson, *J. Appl. Phys.*, **79**, 7991 (1996).
4. B. K. Crone, P. S. Davids, I. H. Campbell, and D. L. Smith, *J. Appl. Phys.*, **84**, 833 (1998).
5. J. Kido and T. Matsumoto, *Appl. Phys. Lett.*, **73**, 2866 (1998).
6. J. Blochwitz, M. Pfeiffer, T. Fritz, and K. Leo, *Appl. Phys. Lett.*, **73**, 729 (1998).
7. T. Matsushima and C. Adachi, *Appl. Phys. Lett.*, **89**, 253506 (2006).
8. J. S. Huang, M. Pfeiffer, A. Werner, J. Blochwitz, K. Leo, and S. Y. Liu, *Appl. Phys. Lett.*, **80**, 139 (2002).
9. H. Ikeda, J. Sakata, M. Hayakawa, T. Aoyama, T. Kawakami, K. Kamata, Y. Iwaki, S. Seo, Y. Noda, and R. Nomura, *SID (The Society for Information Display*, **37**, 923 (2006).
10. T. Matsushima and C. Adachi, *Appl. Phys. Lett.*, **92**, 063306 (2008).
11. C. C. Chang, M. T. Hsieh, J. F. Chen, S. W. Hwang, and C. H. Chen, *Appl. Phys. Lett.*, **89**, 253504 (2006).
12. D. S. Leem, H. D. Park, J. W. Kang, J. H. Lee, J. W. Kim, and J. J. Kim, *Appl. Phys. Lett.*, **91**, 011113 (2007).
13. J. X. Luo, L. X. Xiao, Z. J. Chen, and Q. H. Gong, *Appl. Phys. Lett.*, **93**, 133301 (2008).
14. L. S. Hung, C. W. Tang, and M. G. Mason, *Appl. Phys. Lett.*, **70**, 152 (1997).
15. S. J. Kang, D. S. Park, S. Y. Kim, C. N. Whang, K. Jeong, and S. Im, *Appl. Phys. Lett.*, **81**, 2581 (2002).
16. G. E. Jabbour, B. Kippelen, N. R. Armstrong, and N. Peyghambarian, *Appl. Phys. Lett.*, **73**, 2218 (1998).
17. J. Lee, Y. Park, D. Y. Kim, H. Y. Chu, H. Lee, and L. M. Do, *Appl. Phys. Lett.*, **82**, 173 (2003).
18. K. R. Choudhury, J. H. Yoon, and F. So, *Proc. SPIE*, **6655**, D6551 (2007).
19. V. E. Choong, S. Shi, J. Curless, and F. So, *Appl. Phys. Lett.*, **76**, 958 (2000).
20. H. Ding, K. Park, Y. Gao, D. Y. Kim, and F. So, *Chem. Phys. Lett.*, **473**, 92 (2009).
21. J. Fontanella, C. Andeen, and D. Schuele, *Phys. Rev. B*, **6**, 582 (1972).
22. R. L. Martin, J. D. Kress, I. H. Campbell, and D. L. Smith, *Phys. Rev. B*, **61**, 15804 (2000).
23. M. Lampert and P. Mark, *Current Injection in Solids*, Academic Press, New York (1970).
24. F. C. Wang, S. Liu, and C. L. Zhang, *Microelectron. J.*, **38**, 259 (2007).